

Electronic structure of In_2O_3 from resonant x-ray emission spectroscopy

L. F. J. Piper,^{1,a)} A. DeMasi,¹ S. W. Cho,¹ K. E. Smith,^{1,b)} F. Fuchs,² F. Bechstedt,² C. Körber,³ A. Klein,³ D. J. Payne,⁴ and R. G. Egdell⁴

¹Department of Physics, Boston University, 590 Commonwealth Ave., Boston, Massachusetts 02215, USA

²Institut für Festkörperteorie und-optik and European Theoretical Spectroscopy Facility (ETSF),

Friedrich-Schiller-Universität, Max-Wien-Platz 1, 07743 Jena, Germany

³Institute of Materials Science, Darmstadt University of Technology, Petersenstrasse 23, 64287 Darmstadt, Germany

⁴Chemistry Research Laboratory, Mansfield Road, Oxford OX1 3TA, United Kingdom

(Received 12 November 2008; accepted 20 December 2008; published online 12 January 2009)

The valence and conduction band structures of In_2O_3 have been measured using a combination of valence band x-ray photoemission spectroscopy, O K -edge resonant x-ray emission spectroscopy, and O K -edge x-ray absorption spectroscopy. Excellent agreement is noted between the experimental spectra and O $2p$ partial density of states calculated within hybrid density functional theory. Our data are consistent with a direct band gap for In_2O_3 . © 2009 American Institute of Physics. [DOI: 10.1063/1.3070524]

Indium oxide (In_2O_3) and Sn-doped In_2O_3 are important optoelectronic materials. Early experimental work suggested that In_2O_3 has a direct band gap of 3.75 eV, although a weaker absorption onset at 2.62 eV was also observed and tentatively assigned to indirect transitions.¹ However, *ab initio* band structure calculations have consistently failed to find the pronounced upward dispersion of the topmost valence bands required by the indirect gap hypothesis.^{2,3} The “band gap” of In_2O_3 (presumed to be the lowest energy gap) has therefore been widely quoted to be approximately 3.75 eV, corresponding to the onset of strong optical absorption.⁴ On the other hand, the valence band onset in photoemission experiments on nominally undoped In_2O_3 is found about 2.8 eV below the Fermi level, a value inconsistent with a band gap of 3.75 eV.⁵ Recent theoretical work has shown that the separation between weak and strong optical onsets arises from the fact that transitions from the first six valence bands into the conduction band (CB) are either symmetry forbidden or have very low dipole intensity and has set an upper limit of 2.9 eV for the band gap of In_2O_3 .

We report here a *resonant* x-ray emission spectroscopy (RXES) study of the electronic structure of In_2O_3 . This technique involves coupled x-ray absorption and x-ray emission processes and is used here to investigate the O $2p$ partial density of states (PDOS), below and above the Fermi level of In_2O_3 . RXES was also used to probe the bulk valence band dispersion of In_2O_3 . We directly compare the experimental spectra with hybrid density functional theory (DFT) calculations of the band structure. We find excellent agreement between the x-ray absorption and emission spectra and the calculated O $2p$ PDOS. Furthermore, examination of the resonant emission spectra provides evidence of a lack of an indirect band gap, in agreement with the DFT calculations.

In_2O_3 thin films were grown by radio frequency magnetron sputtering onto doped Si substrates to a thickness of 400–500 nm using pure Ar as the sputter gas and a 400 °C substrate temperature. Carrier concentrations were estimated as $n=3 \times 10^{19} \text{ cm}^{-3}$ from transport measurements. The

samples were ultrasonically cleaned in acetone and then transferred into the ultrahigh vacuum spectrometer chamber base pressure of 1×10^{-10} torr. The experiments were performed at the undulator beamline X1B at the National Synchrotron Light Source at Brookhaven National Laboratory. This beamline is equipped with a spherical grating monochromator. The absorption spectra were recorded in the total electron yield mode by measuring the sample drain current. During the x-ray absorption spectroscopy (XAS) measurements, the entrance and exit slits of the monochromator were set to a width of 20 μm , corresponding to an energy resolution of approximately 0.20 eV for an incident photon energy of 530 eV (the O K -edge region). The current from a gold mesh placed in the incident beam was used to measure the incident flux and subtract any variations in sample drain current related to the beamline optics rather than the sample electronic structure. The photon energy was calibrated to the O K edge and Ti L edge from rutile TiO_2 measured during the experiment.⁶ The emission spectra were recorded using a Nordgren-type grating spectrometer, with a total instrumental resolution of 0.37 eV for above-threshold XES at the O K edge.⁷ The measurements were taken in a specular geometry. The monochromator slits were set to 70 μm during the RXES measurements (energy resolution of 0.65 eV). Core-level x-ray photoemission spectroscopy (XPS) was also performed at X1B using a SCIENTA-100 hemispherical electron energy analyzer. A 30 min Ar^+ ion sputtering cycle (500 V, 25 mA, and 5×10^{-5} torr) was employed to clean the sample. The core-level XPS revealed no C $1s$ signal above background following the sputtering cycle. Core-level O $1s$ and In $4d$ energy axes were calibrated to the Fermi energy (E_F) and binding energies of the $4f$ states of a Au foil in contact with the sample (not shown here) in order to plot the XES and XAS on a common binding energy scale. For direct comparison with the O K -edge XES and theoretical computations, XPS of the semicore In $4d$ and valence band (VB) region of these films was also measured using a Al $K\alpha$ x-ray source ($h\nu=1486.6$ eV) and SCIENTA-300 spectrometer (effective instrumental resolution of 300 meV) at the National Centre for Electron Spectroscopy and Surface Analysis (NCESS), UK.

^{a)}Electronic mail: lfjpiper@buphy.bu.edu.

^{b)}Electronic mail: ksmith@bu.edu.

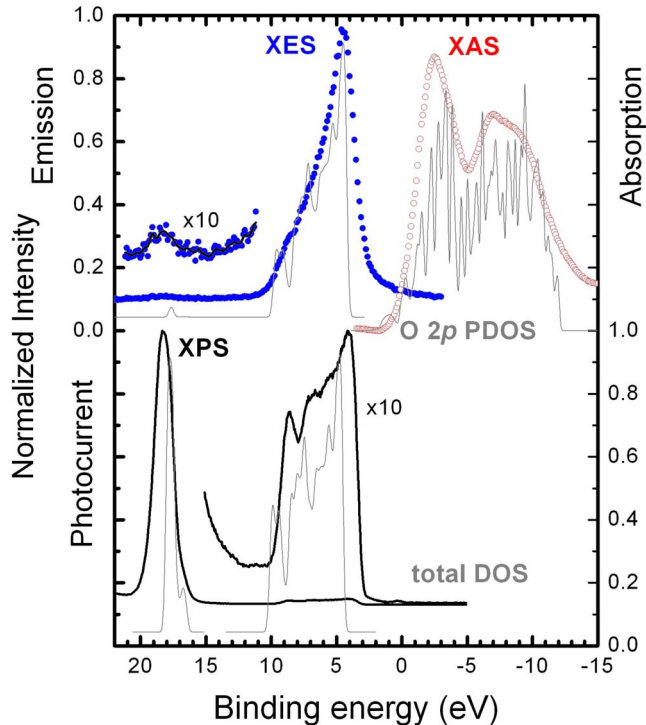


FIG. 1. (Color online) (Top panel) The O K -edge XES (blue filled circles) and O K -edge XAS (empty red circles) are plotted on a common binding energy axis. Emission from In $4d$ -O $2p$ hybrid states is visible around 18 eV, and this region of the XES is magnified ten times for clarity. A three-point binomial smooth is included on the magnified XES as a guide to the eye. Also plotted is the broadened DFT+HSE03 O $2p$ PDOS. (Bottom panel) XPS ($h\nu=1486.6$ eV) of the In $4d$ shallow core level and the VB is shown along with the broadened calculated occupied total DOS.

Band structure calculations of bcc bixbyte structure $Ia\bar{3}$ In_2O_3 were performed within the framework of hybrid DFT using the recently proposed HSE03 functional for exchange and correlation.⁸ All the calculations are performed using the Vienna *ab initio* simulation package (VASP), and the projector augmented wave (PAW) method has been used to model the electron-ion interaction. The hybrid functionals allow for an approximate treatment of the quasiparticle effects, while the PAW method yields all-electron wave functions. Further details can be found elsewhere.³

Figure 1 presents (i) the O K -edge XES spectrum recorded with excitation energies above the absorption threshold, (ii) the O K -edge XAS spectrum, and (iii) the valence band (VB) XPS spectrum, all plotted on a common binding energy scale. The XPS spectrum agrees with recent measurements of high quality $\text{In}_2\text{O}_3(100)$ samples reported elsewhere.⁹ We note that the location of the valence band peak (~ 4.5 eV below E_F) for both XES and XPS are in agreement. We observe a peak in the O $K\alpha$ XES spectrum at 17 eV below E_F . This lies at the binding energy of the In $4d$ shallow core level and is due to In $4d$ -O $2p$ hybridization. The sensitivity of XES to hybridized states has been well established in metal oxides.¹⁰

Also included in Fig. 1 is the computed total DOS and O $2p$ PDOS of bixbyte In_2O_3 , calculated within the DFT-HSE03; these are plotted below VB-XPS and the normalized O K -edge XES and XAS spectra, respectively. The occupied and unoccupied contributions were first convoluted separately with a Gaussian with widths of 0.37 and 0.20 eV, respectively, corresponding to the experimental energy reso-

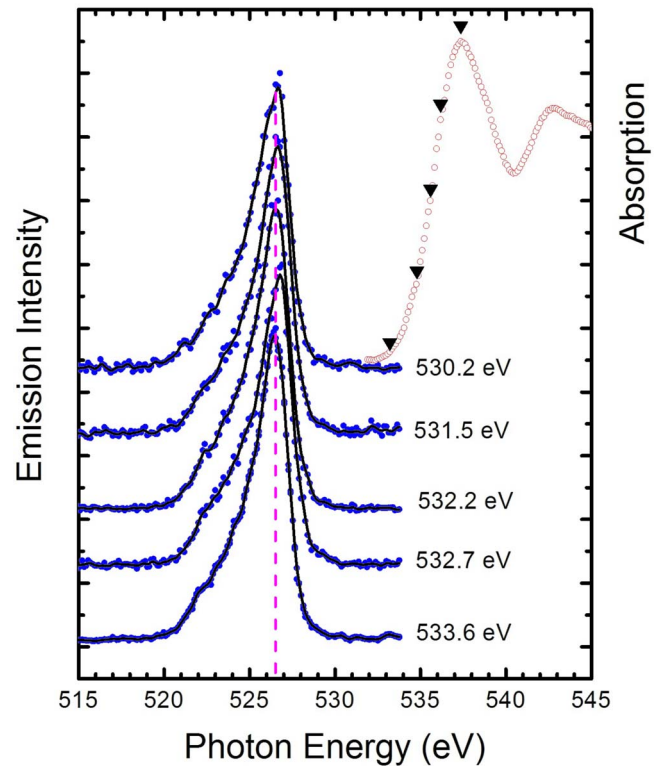


FIG. 2. (Color online) O K -edge RXES (blue filled circles) vertically offset as a function of excitation energy. The corresponding XAS spectrum (red open circles) is also included; the excitation energies for the RXES spectra are marked on the XAS spectrum with triangles. The vertical line in the RXES spectra is a guide to the eye.

lutions of the XES and XAS spectra. This enabled a fairer comparison with the experimental spectra. To obtain a common binding energy axis, the O $2p$ PDOS was then rigidly shifted to match the VB peaks of both the XPS and XES. An additional shift of -1 eV was required for the unoccupied PDOS due to the influence of the core hole with the final state of the XAS process, providing an estimate of the core-hole binding energy. The experimental spectra are well reproduced by the first principles calculation, most notably: the location of the calculated In $4d$ -O $2p$ hybrid states and the XAS spectral shape.

For weakly correlated systems and excitation energies close to the absorption edge, resonance effects are known to influence the shape of the emission spectra due to k -selectivity.^{11,12} As a result, it is possible to evaluate the nature of the band gap and VB dispersion with RXES. For instance, RXES spectra of GaN,¹³ InN,¹⁴ and ZnO (Ref. 15) are consistent with direct band gaps and a VB which disperses downward in moving away from Γ , while RXES of CdO is consistent with an indirect band gap and an upward dispersing VB.¹⁶ Figure 2 displays the raw RXES spectra of the O K edge of In_2O_3 , as a function of incident energy. As the incident energy is increased from the absorption onset to the main absorption peak, little or no change in the corresponding emission spectra is observed. This is in contrast to the RXES spectra from the direct gap materials GaN, InN, and ZnO, where clear changes in the spectral shape and XES peak positions are observed.¹³⁻¹⁵

Figure 3(a) displays the emission spectra for incident energies of $h\nu=530.2$ eV and 545.0 eV. These excitation energies correspond to the onset of O K -edge absorption and

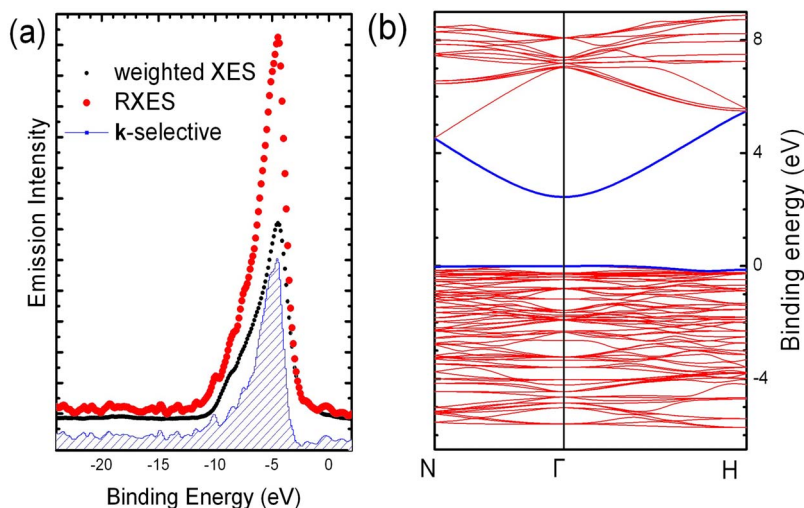


FIG. 3. (Color online) (a) O K -edge spectra recorded at the absorption onset ($h\nu_{\text{excite}}=530.2$ eV) and above threshold ($h\nu_{\text{excite}}=545.0$ eV). The coherent contribution of the $h\nu=530.2$ eV RXES spectrum is also plotted (red filled area). (b) The DFT+HSE03 calculated band structure along the N - Γ - H high symmetry points of bcc In_2O_3 , the topmost VB and lowest CB are highlighted (blue) for clarity.

well above the absorption threshold, respectively. The emission spectra were also divided by E^3 (where E is the photon energy) to correct for the photon density of states' contribution to the transition rate.¹⁷ The above-threshold emission spectrum corresponds to the incoherent contribution. If this is subtracted from the threshold emission spectrum, the difference is then the coherent contribution to the RXES. (The above-threshold emission spectrum was weighed to ensure the largest non-negative sum difference between the onset and above-threshold emission spectra.¹¹) This difference spectrum is also plotted in Fig. 3(a). Figure 3(b) displays the DFT+HSE03 band structure near the Brillouin zone center of bcc In_2O_3 (N - Γ - H high symmetry points). The onset of the absorption spectrum corresponds to the CB maximum, which lies at the zone center (i.e., the Γ -point). As a result, the coherent \mathbf{k} -selective contribution to the onset RXES spectrum corresponds from the Γ -point. No difference is observed between the spectral shape and energetic position of the coherent RXES (near the Γ -point) and the above-threshold XES. Referring to the DFT in Fig. 3(b), this is consistent with the VB maximum (VBM) being located at the zone center. We note that this finding is in contrast to our results from CdO which has an indirect gap, where the combination of the pd -repulsion and crystal symmetry results in a significant difference between the VBM and VB near the Γ -point.¹⁶

In conclusion, the electronic structure of In_2O_3 has been investigated by XES, XAS, XPS, and RXES. Direct comparison between the O K -edge XES and XAS, and the hybrid DFT calculated O $2p$ PDOS reveals excellent agreement in terms of the spectral shape and the relative peak positions. The O K -edge RXES results experimentally rule out the possibility of an indirect band gap.

The Boston University (BU) program is supported in part by the Department of Energy under Grant No. DE-FG02-98ER45680 and in part by the Donors of the American Chemical Society Petroleum Research Fund. The BU RXES spectrometer system was funded by the U.S. Army Research Office under Grant Nos. DAAD19-01-1-0364 and DAAH04-95-0014. The National Synchrotron Light Source, Brookhaven National Laboratory, is supported by the U.S. Department of Energy, Office of Science, Office of Basic Energy Sciences, under Contract No. DE-AC02-

98CH10886. The NCESS facility is supported by the EPSRC-GB, U.K., under Grant No. GR/S94148. Financial support is also acknowledged from the European Community in the framework of the network of excellence NANOQUANTA (Contract No. NMP4-CT-2004-500198) and the Deutsche Forschungsgemeinschaft (Project No. Be1346/18-2).

- ¹R. L. Weiher and R. P. Ley, *J. Appl. Phys.* **37**, 299 (1966).
- ²P. Erhart, A. Klein, R. G. Egdell, and K. Albe, *Phys. Rev. B* **76**, 174116 (2007).
- ³F. Fuchs and F. Bechstedt, *Phys. Rev. B* **77**, 155107 (2008).
- ⁴I. Hamberg, C. G. Granqvist, K. F. Berggren, B. E. Sernelius, and L. Engstrom, *Phys. Rev. B* **30**, 3240 (1984).
- ⁵A. Walsh, J. L. F. Da Silva, S.-H. Wei, C. Korber, A. Klein, L. F. J. Piper, A. DeMasi, K. E. Smith, G. Panaccione, P. Torelli, D. J. Payne, A. Bourlange, and R. G. Egdell, *Phys. Rev. Lett.* **100**, 167402 (2008).
- ⁶X. Chen, P.-A. Glans, X. Qiu, S. Dayal, W. D. Jennings, K. E. Smith, C. Burda, and J. Guo, *J. Electron Spectrosc. Relat. Phenom.* **162**, 67 (2008).
- ⁷J. Nordgren, G. Bray, S. Cramm, R. Nyholm, J. E. Rubensson, and N. Wassdahl, *Rev. Sci. Instrum.* **60**, 1690 (1989).
- ⁸J. Heyd, G. E. Scuseria, and M. Ernzerhof, *J. Chem. Phys.* **118**, 8207 (2003).
- ⁹A. Bourlange, D. J. Payne, R. G. Egdell, J. S. Foord, P. P. Edwards, M. O. Jones, A. Schertel, P. J. Dobson, and J. L. Hutchison, *Appl. Phys. Lett.* **92**, 092117 (2008).
- ¹⁰D. J. Payne, R. G. Egdell, A. Walsh, G. W. Watson, J. Guo, P. A. Glans, T. Learmonth, and K. E. Smith, *Phys. Rev. Lett.* **96**, 157403 (2006); P.-A. Glans, P.-A. Glans, T. Learmonth, C. McGuinness, K. E. Smith, J. Guo, A. Walsh, G. W. Watson, and R. G. Egdell, *Chem. Phys. Lett.* **399**, 98 (2004); P.-A. Glans, T. Learmonth, K. E. Smith, J. Guo, A. Walsh, G. W. Watson, F. Terzi, and R. G. Egdell, *Phys. Rev. B* **71**, 235109 (2005); C. McGuinness, C. B. Stagaescu, P. J. Ryan, J. E. Downes, D. Fu, and K. E. Smith, *ibid.* **68**, 165104 (2003).
- ¹¹S. Eisebitt and W. Eberhardt, *J. Electron Spectrosc. Relat. Phenom.* **110**, 335 (2000).
- ¹²A. Kotani and S. Shin, *Rev. Mod. Phys.* **73**, 203 (2001).
- ¹³V. N. Strocov, T. Schmitt, J. E. Rubensson, P. Blaha, T. Paskova, and P. O. Nilsson, *Phys. Rev. B* **72**, 085221 (2005).
- ¹⁴L. F. J. Piper, L. Colakerol, T. Learmonth, P.-A. Glans, K. E. Smith, F. Fuchs, J. Furthmuller, F. Bechstedt, T.-C. Chen, T. D. Moustakas, and J.-H. Guo, *Phys. Rev. B* **76**, 245204 (2007).
- ¹⁵A. R. H. Preston, B. J. Ruck, L. F. J. Piper, A. DeMasi, K. E. Smith, A. Schleife, F. Fuchs, F. Bechstedt, J. Chai, and S. M. Durbin, *Phys. Rev. B* **78**, 155114 (2008).
- ¹⁶L. F. J. Piper, A. DeMasi, K. E. Smith, A. Schleife, F. Fuchs, F. Bechstedt, J. Zuniga-Perez, and V. Munoz-Sanjose, *Phys. Rev. B* **77**, 125204 (2008).
- ¹⁷W. L. O'Brien, J. Jia, Q.-Y. Dong, T. A. Callcott, D. R. Mueller, D. L. Ederer, and C.-C. Kao, *Phys. Rev. B* **47**, 15482 (1993).